China Fucheng1 SAR support in GAMMA Software

Urs Wegmüller, Christophe Magnard, Gamma Remote Sensing AG

Version 29-May-2024

1. INTRODUCTION

In this document the support provided in the GAMMA Software for the processing of data of the Chinese C-band SAR Fucheng1 is summarized. The first Fucheng1 SAR was launched in June 2023. Fucheng-1 is an interferometric imaging synthetic aperture radar (SAR) remote sensing satellite for the six-satellite Mianyang constellation.

In Section 2 the importing of the Fucheng1 SLC data is described, followed by an assessment of the data characteristics, in Section 3. In Section 4, the DInSAR processing sequence for repeat pass interferometric data pairs acquired by Fucheng1 with a 11-day time interval and related results are presented.

2. IMPORTING LT1 SLC DATA

2.1.Importing SLC data

Fucheng1 SLC data are provided as a GeoTIFF with meta data in XML format, that can be read / imported using the program ***par_Fucheng_SLC***.

par_Fucheng_SLC bc3-sm-slc-vv-20240103t031850-003378-000018-000d32-01.tiff bc3-sm-slc-vv-20240103t031850-003378-000018-000d32-01.xml calibration-bc3-sm-slc-vv-20240103t031850-003378-000018-000d32-01.xml - 20240103.slc.par 20240103.slc 0 2.

As input, the GeoTIFF and the meta data XML files are indicated. The program generates the SLC binary data file, in SCOMPLEX or FCOMPLEX format, and the related SLC parameter file. The SLC can be visualized using

disSLC 20230403.slc 12426 1 - 1. .35 0

and the spectrum can be checked using

dismph_fft 20230403.slc 12426 1 0 1. .35 128 3 0

The orbit state vectors were checked using the program *ORB_filt_spline.py* – and found not to be "noisy". Possibly, the state vectors have been adequately processed and do not correspond to the unfiltered on-board GNSS measurements.

/bin/cp 20230403.slc.par 20230403.slc.par.orig

ORB_filt_spline.py 20230403.slc.par.orig 20230403.slc.par --png png_dir --degree 5

The statistics show standard deviation values of the unfiltered state vector positions from the filtered solution below 1.2mm.

Using the SLC we generate a backscatter image in slant range geometry using
multi_look 20230403.slc 20230403.slc.par 20230403.mli 20230403.mli.par 5 5
ras_dB 20230403.mli 2485 1 - 1 1 -22.5 3.5 gray.cm 20230403.mli.bmp 0 1
A section of a resulting Fucheng1 backscatter image is shown in Figure 1.



Figure 1 Section of Fucheng1 data (2 x 2 look MLI in slant range geometry) over Rovinari, Rumania.

2.2.Importing detected data in slant range geometry

Not available so far.

2.3.Importing geocoded / georeferenced data

Not available so far.

3. ASSESSMENT OF SOME CHARACTERISTICS OF LT1 STRIPMAP SLC

3.1.Radiometric calibration and estimation of NESZ

We were (so far) not able to check the absolute radiometric calibration for Fuching1 data with know target such as corner reflectors or transponders. When reading the data we also read the available calibration data and apply it. The signal level of the resulting SLC (in FCOMPLEX data) looks correct. No validation with different satellite data or targets with known backscatter coefficients was done in our assessment.

Using dark areas (radar shadow and smooth water surfaces) we estimated a Noise Equivalent Sigma Zero value. The NESZ value is low (< -20 dB).

3.2.Point target characteristics

Considering several small, strong scatterers present in the scene we determined the following point target characteristics:

slant range resolution (3dB):	1.7 m
azimuth resolution (3dB):	2.8 m
peak_side_lobe_ratio:	< -22 dB

3.3.Geocoding

We generated a multi-look intensity image using 2 range and 2 azimuth looks and conducted a geocoding sequence, using the 1-arc-second Copernicus DEM. As part of the geocoding sequence a refinement was determined based on the offset between a simulated backscatter image (calculated based on the orbit data and the DEM) and the actual SAR backscatter.

The refinement statistics indicate for the offset estimates a very small standard deviation of below 2.5 multi-look pixel in both slant range and azimuth directions with an estimated refinement correction below 50m. Geocoded results are shown in Section 4.

3.4. RFI filtering

The Fucheng1 SLC data over Tianjin, China was affected by Radio-Frequency-Interference (RFI). Some areas show strong image anomalies with an anomalous spectrum. So the RFI is not caused by a narrow band microwave transmitter, but by a broader signal, maybe a chirp of a radar. In the data over Rumania we did not observe this problem. So it is rather likely that external RFI and not internal problems such as cross-talk, or processing issues are the cause. Figure 2 shows the distortion and the related spectrum when displaying the SLC with dismph_fft. We were not able to remove these distortions.

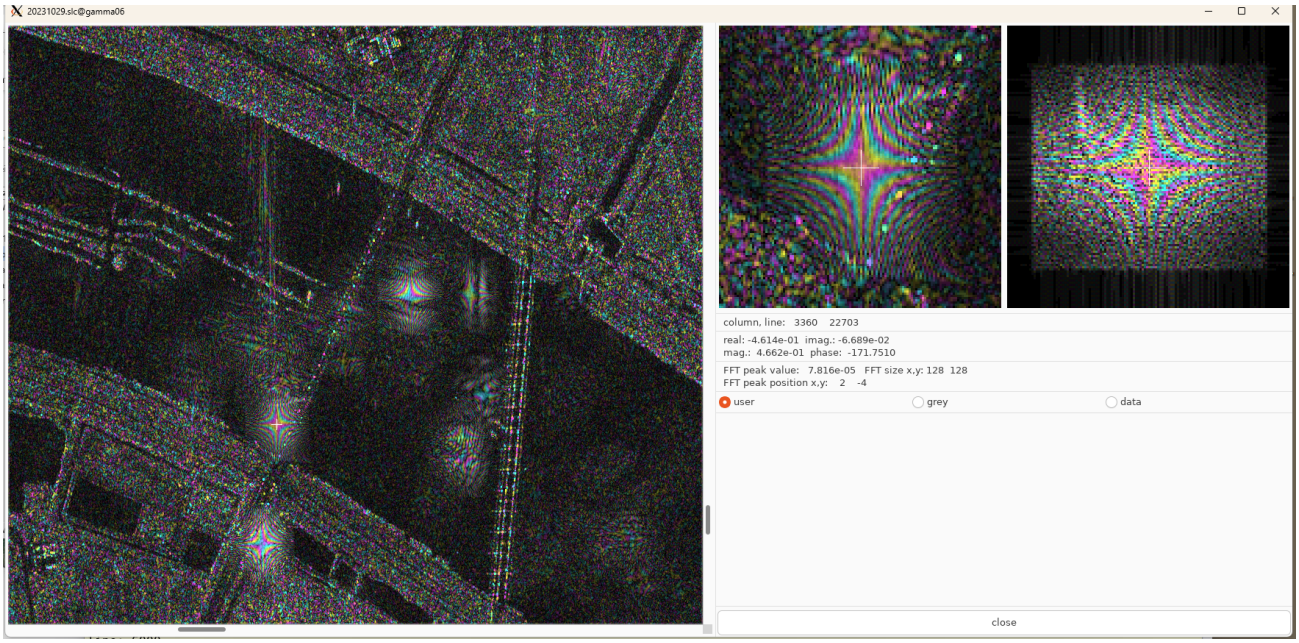


Figure 2 Section of Fucheng1 SLC showing the RFI anomalies observed in the data over Tijanjin, China. In the SLC there are anomalous bright areas with a distinct phase pattern. The spectrum shows a similar pattern as the image. The image to the left shows an image section (brightness for intensity and color for phase). The two smaller images to the right show the zoom on the cursor location (left) and the spectrum at that location (right).

4. FUCHENG1 REPEAT-PASS DIFFERENTIAL SAR INTERFEROMETRY (DINSAR)

4.1. Processing sequence used

We were able to test Fucheng1 differential SAR interferometry using data stacks over Tianjin, China and over a mining area in Romania. A flow chart of the processing sequence used is shown in Figure 3. In the following, some of the steps are further discussed.

In the case of the data over Romania we selected the first scene, acquired on 1-Oct-2023 as the reference, generated a multi-look intensity image (MLI) with 2 range and 2 azimuth looks, and conducted a geocoding sequence using the Copernicus 30m global DEM. This also included the resampling of the DEM height into the MLI geometry.

Next, we co-registered the second SLC to the reference SLC. In this we used a sequence that also considers the terrain height (using *rdc_trans*). In this a refinement is done using intensity matching, to achieve a co-registration accuracy better than 0.12 SLC pixel.

The repeat interval of Fucheng1 is 11 days. The orbit geometry is accurately maintained, so that almost all perpendicular baselines were below 100m.

Then we calculated the orbital and topographic phase (*phase_sim_orb*) and the differential interferogram (*SLC_diff_intf*). With few exceptions (probably related to strong precipitation) the

differential interferograms include areas with high coherence. Many of the differential interferograms shows a quite substantial overall phase trend. We unwrap the differential interferogram, estimate the overall phase trend (*quad_fit*), and subtract it (*sub_phase*), to get the "detrended" differential interferogram.

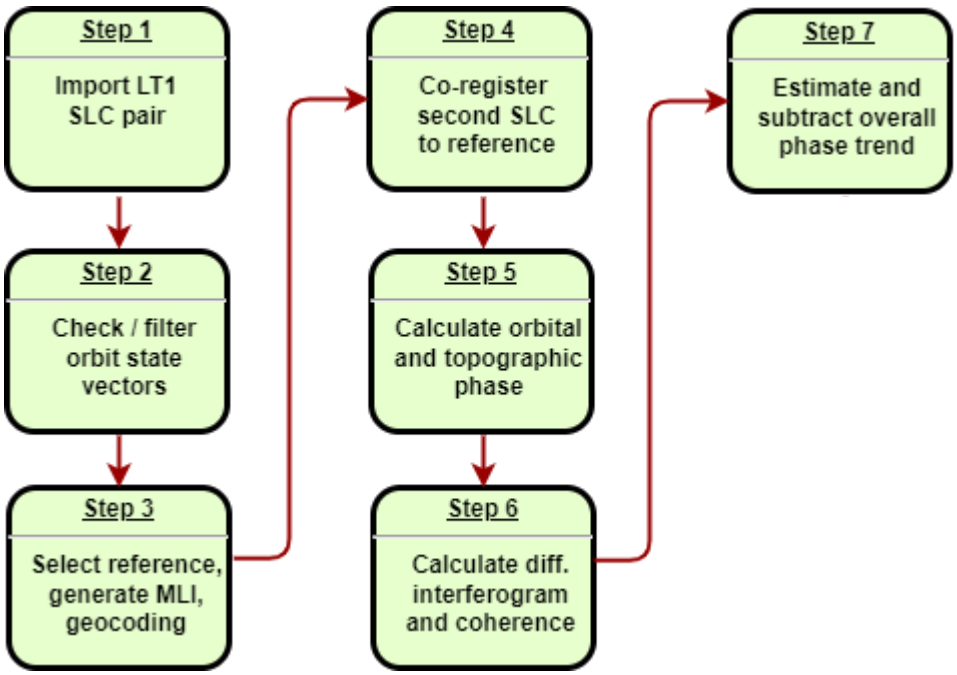
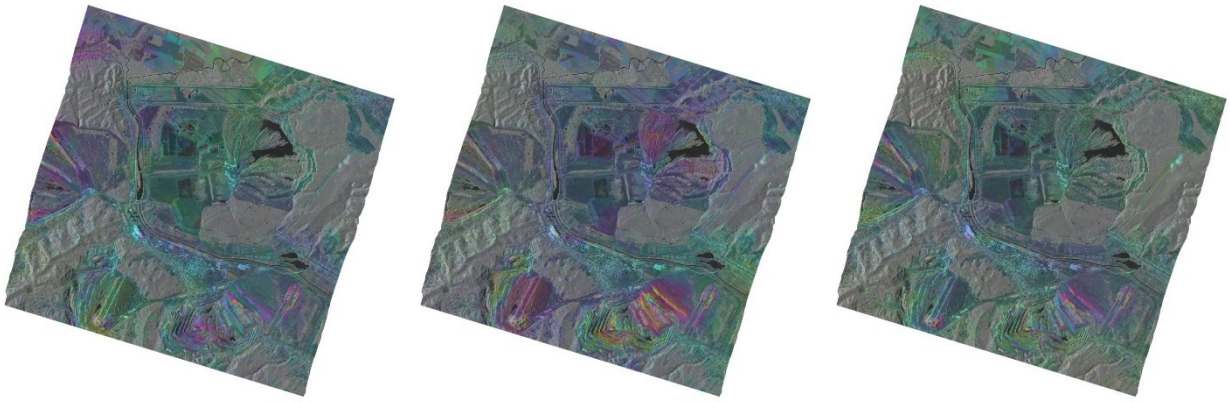


Figure 3 Flowchart of DInSAR processing sequence used.

Figure 4 shows for a small section that includes the village Rovinari, a coal power plant, open pit and deposit areas. Some areas show cm scale subsidence even over 11 day intervals. These are compacting deposit areas. In the mining area we also observe some local fast displacements. In other areas the signal is decorrelated because of the changes to the ground surface. The multi-temporal coherence RGB image in Figure 5 shows that the mining areas are in some intervals coherent (no surfaces change) and in other intervals decorrelated (surface change), resulting in different colors. Similarly multi-temporal backscatter images can be considered to observe temporal change (Figure 6).

Figure 7 shows the Fucheng1 coherence product for October 2023. It supports recognizing landuse classes.



a) 20231001_20231012 b) 20231012_20231023 c) 20231023_20231103

Figure 4 "Detrending" Fucheng1 differential interferogram for subsequent 11-day intervals in 2023. One color cycle corresponds to 2π interferometric phase (corresponding to 2.78cm of line-of-sight displacement).

4.2. Discussion

The Romania example investigated clearly confirms that Fucheng1 data has a good potential for interferometry. Considering the short spatial baselines and consistent signal quality it is also clear that the data will support conducting an interferometric time series analysis (PSI, SBAS, etc.), e.g. using the IPTA software.

Thanks to the 11-day time interval and the relatively short spatial baselines (mostly < 100m) the coherence of the interferograms is generally high, except for areas with significant changes (water surfaces, forest, fields which are cultivated, areas where the surface was mined or where material was deposited during the interferometric time interval).

The differential interferograms confirm that the data is suited for displacement mapping. A fast-moving landslide could be identified, mapped and an approximate velocity could be estimated.

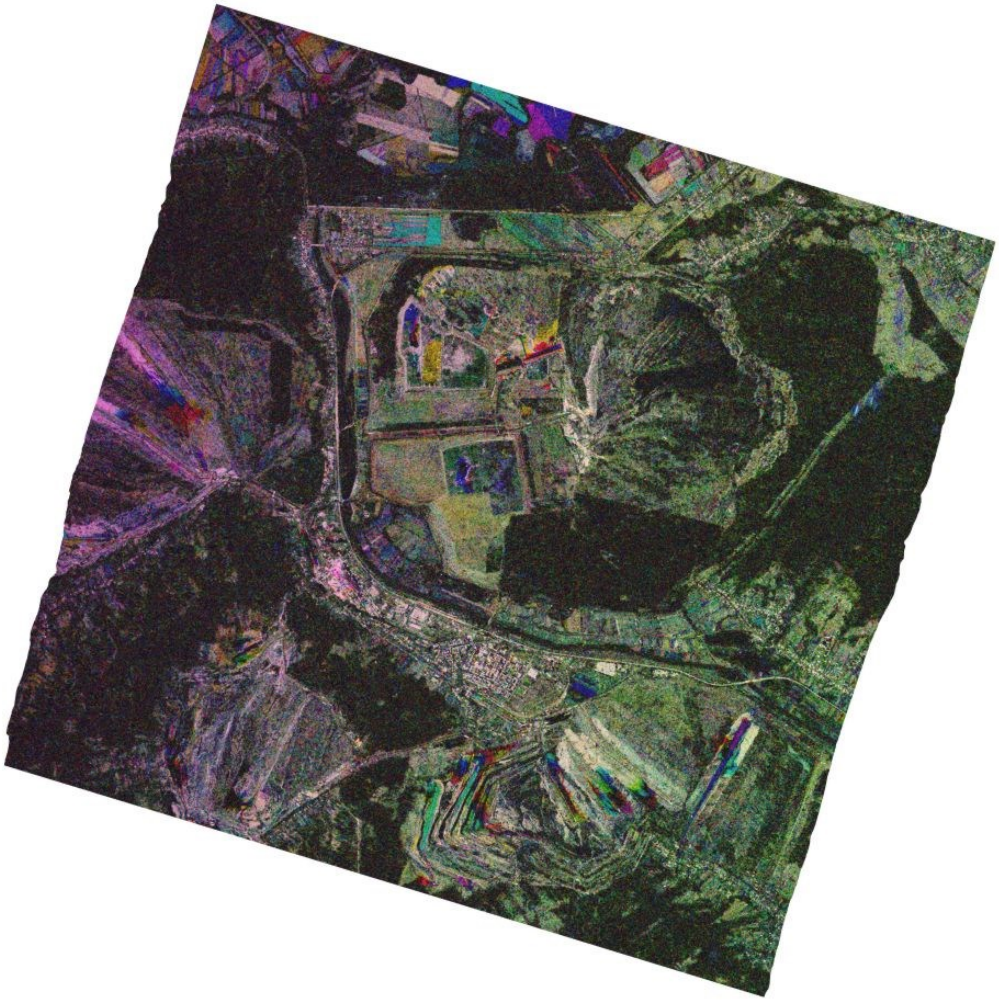


Figure 5 Multi-temporal coherence image. Red: 20231001_20231012, Green: 20231012_20231023, Blue: 20231023_20231103.

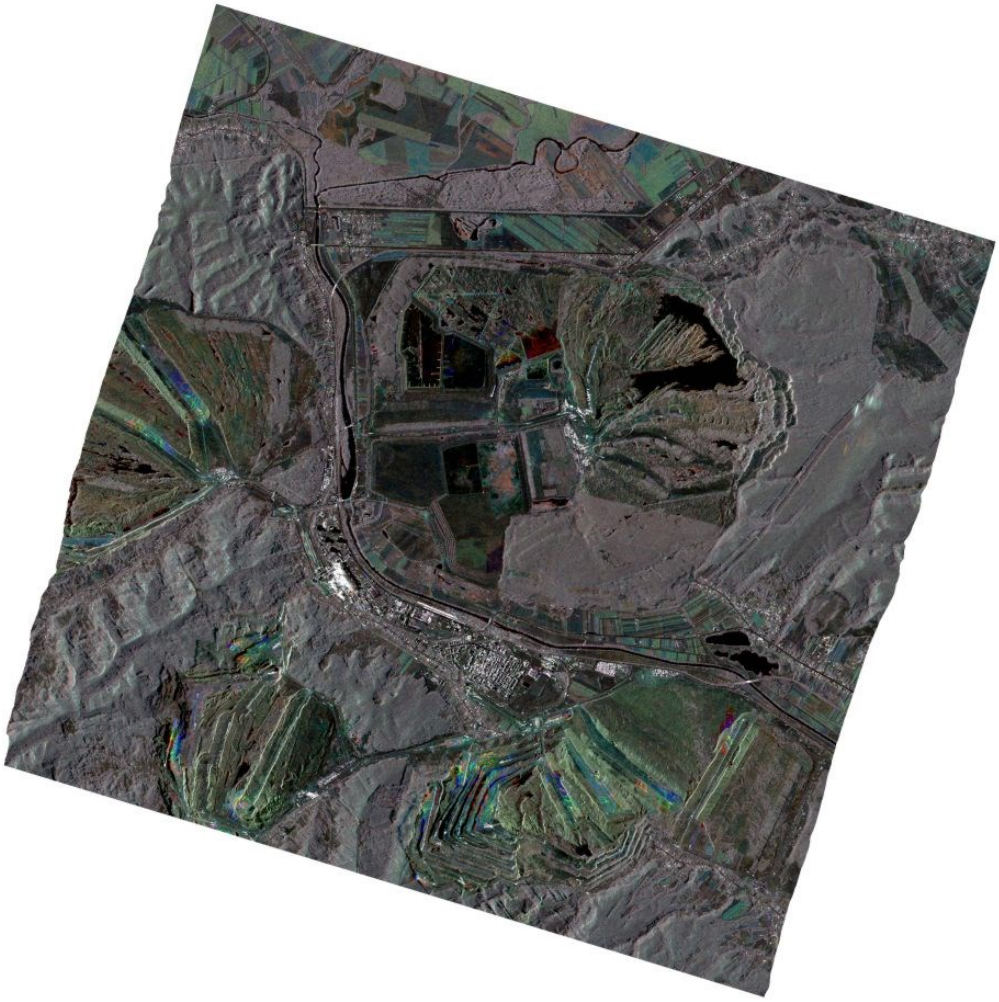


Figure 6 Multi-temporal backscatter composite (Red: fall 2023, green: winter 2023/2024, blue (early spring 2024).

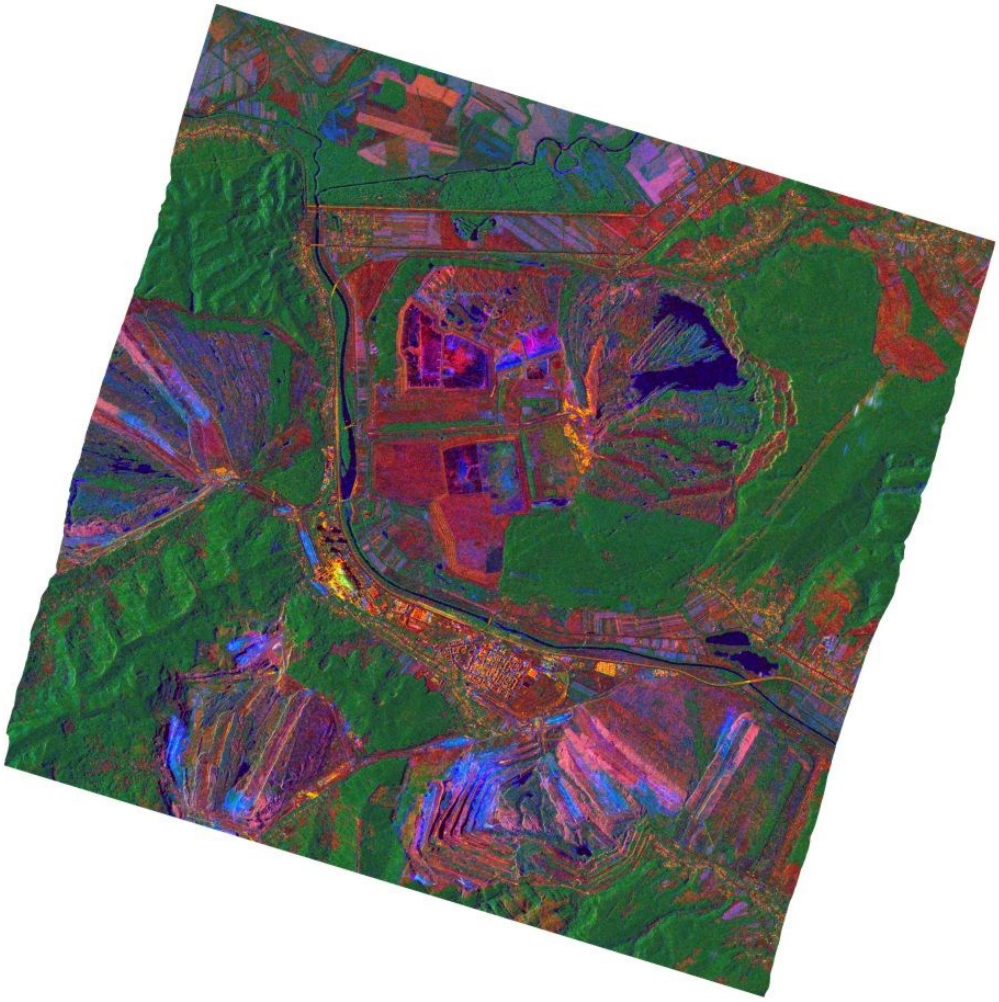
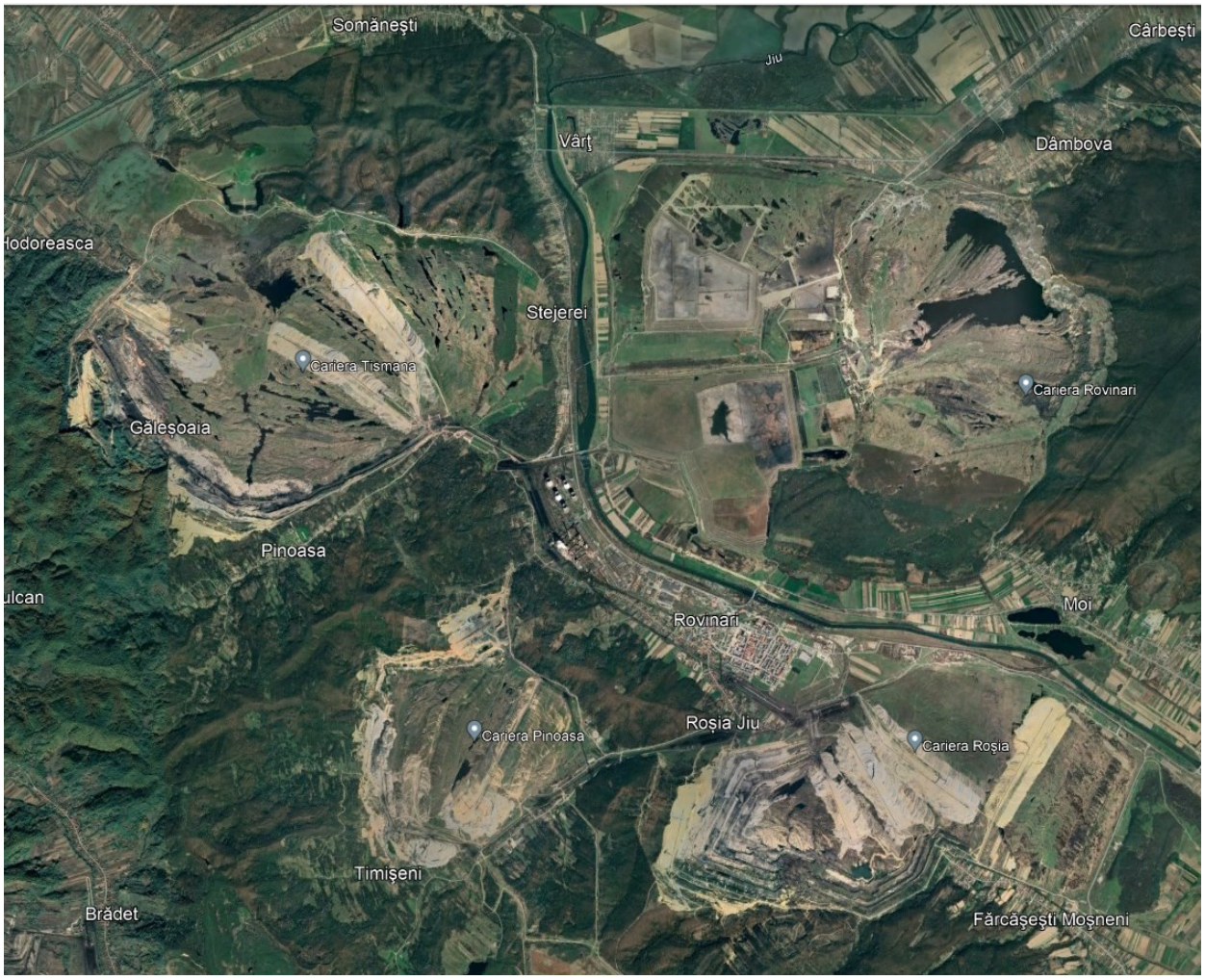


Figure 7 Fucheng1 coherence product for October 2023. Red: average coherence over 3 11-day interferograms of Figure 4; green: average backscatter; blue: backscatter temporal variability. Green areas correspond mainly to forest, blue ones to water or other areas with low coherence, low backscatter and high backscatter variability.

5. ACKNOWLEDGMENT AND COPYRIGHTS

XingGuo Chen, Beijing Di Kong Software Technology Co., Ltd, is acknowledged for providing access to the Fucheng1 data used. Below some images extracted from Google Earth are added.

Appendix 1: Some images from the Rovinari area extracted from Google Earth.







Appendix 2: The descending orbit ground-motion information in the European Ground Motion Service for the Rovinari area.

